Journal of Scientific Research & Reports

27(2): 37-51, 2021; Article no.JSRR.66402
ISSN: 2320-0227

Diurnal Wind Pattern and Climate Condition on the Coastal Region of Qatar

Yuan Li[1] and Reza Sadr[1*]

[1]Department of Mechanical Engineering, Texas A and M University, TX, 77843, College Station, United States.

Authors' contributions

This work was carried out in collaboration between both authors. Author YL is the PhD student in charge of data analysis. Author RS supervised the experimental campaign and the data analysis. Both authors read and approved the final manuscript.

Article Information

DOI: 10.9734/JSRR/2021/v27i230357
Editor(s):
(1) Dr. Rahul Kumar Jaiswal, National Institute of Hydrology, India.
Reviewers:
(1) Ahmed N. Abdalla, Huaiyin Institute of Technology, China.
(2) K. V. Subrahmanyam, Vikram Sarabhai Space Centre (VSSC), India.
Complete Peer review History: http://www.sdiarticle4.com/review-history/66402

Original Research Article

Received 12 January 2021
Accepted 18 March 2021
Published 26 March 2021

ABSTRACT

Climate pattern in the Persian Gulf is of great interest due to the strategic geographical location of the gulf as a waterway of major oil transportation and its increasing regional economic importance. However, long term and continues climate observations in this region are rare, especially for high resolution data. High resolution wind pattern and climate conditions were measured at 3 heights on a 9 m tower on the shoreline north of Qatar (26.08 N, 51.36 E) from August 2015 to September 2016. In this work, the annual wind and climate patterns (wind velocity, temperature, relative humidity, and air pressure) are first presented. Drag coefficient, turbulent kinetic energy and sensible heat flux are calculated using the high speed measured data to explain the observed climate pattern. The results show the wind in the southern part of the gulf is dominant by a northwest stream with a diurnal average speed of 4.7 m/s. During the test year, the diurnal average temperature and relative humidity were 27°C and 70%, respectively. The drag coefficient is much higher for the wind from 270^{o}-330^{o}, corresponding to the wind coming mainly from northwest. The Turbulent Kinetic Energy (TKE) is strong during the daytime, especially around noon when the diurnal value is at its peak, and weak during the night. The result of this analysis may be used for better understanding of the local climate, allowing for further assessment of wind energy and pollution diffusion in the region.

**Corresponding author: E-mail: reza.sadr@tamu.edu;*

Keywords: Climate pattern; wind energy; TKE; heat flux.

1. INTRODUCTION

Weather Research and Forecasting (WRF) models are of growing interest for the purpose of studying air pollution, air quality, and wind energy assessment, among others. Availability of accurate lower atmospheric data such as wind speed, direction, temperature, and atmospheric turbulence are important parts of WRF model development [1]. The predictions of low wind speed frequencies, for example, have important applications in air pollution analysis, while the predictions of high wind speed frequencies have important applications in the areas of structural design and assessment of potential wind power generator output [2,3]. Further, turbulent kinetic energy and sensible heat flux are commonly investigated for better understanding of the physics of atmospheric transportation and climate condition as well as to help develop climate models [4,5,6]. Finally, knowledge of diurnal ambient temperature, relative humidity, and air pressure are also used when evaluating local climate conditions [7,8,9,10]. In brief, regional annual climate characterization, along with atmospheric turbulent kinetic energy (TKE) and turbulent heat flux (THF) measurement is of special importance in evaluating and improving WRF models.

The Persian Gulf (the Gulf) is a Mediterranean Sea between Iran and the Arabian Peninsula, surrounded by natural geologic formations that contain two-thirds of the world's proven oil reserves and one-third of the world's proven natural gas reserves [11,12,13]. The global transport of oil and gas makes the Gulf one of the most important waterways in the world that has motivated observation and simulation of the climate conditions in this region in recent years [14-20]. Further, due to its long record of pollution and concerns about greenhouse gases and climate change, there is a growing interest in this region for development of renewable energy. The ability to harvest and utilize energy from renewable sources is sensitive to regional climate conditions as well as climate change, requiring further study of local climate and wind patterns for a specific location of interest [21]. For example, Yip et al. [22] investigated the potential for wind energy in the Arabian Peninsula, concluding that the wind resource in the coastal area along the Persian Gulf is more variable than that of the Red Sea at a similar latitude. More persistent wind was also found along the coast of the Arabian Gulf, lending itself for wind energy applications. Qatar is a peninsula on the south part of the Persian Gulf. The climate of Qatar is a subtropical and hot desert climate with low annual rainfall and extremely hot summers. The annual mean rainfall is 75 mm that is mostly in the wintertime [20]. A strong wind, called Shamal, blows hot and dry air from the northwest, Iraq, in summer [23] while in winter it can brings strong sandstorms [24,18].

A feasibility study of any wind energy conversion system includes the study of spatial, temporal, and directional wind speed variation that requires consistent seasonal measurements of the wind speed and direction. Reliable annual, monthly, daily, and even hourly frequency distributions of wind data are required in order to optimize wind energy conversion systems and energy extraction [25]. Meanwhile, most studies focus on the inland locations in this region, e.g., Saudi Arabia and Iran [15,8,22], with only a few studies for coastal regions in Bahrain and Qatar [26,27,28]. High resolution data is even more rare around the Gulf as the existing studies are often obtained from weather station or satellite data with low temporal resolution [14,29]. More importantly, most available observations in the Arabian Peninsula are sparse in space and inconsistent in time, spatially scattered observations with varying record lengths [30,22].

In this work, high frequency atmospheric data collected from August 2015 to September 2016 using a state-of-the-art tower located in the coastal region of Qatar is presented and discussed. The annual climate pattern along with basic atmospheric turbulence characteristics are presented here for the first time to better facilitate understanding of the regional climate condition and pollution dispersion, as well as to be used in an initial assessment for wind energy potential. Basic theory on the data processing is introduced in section 2. Experimental site and instruments used are introduced in section 3. Diurnal climate indices (wind velocity/direction, temperature, relative humidity, and air pressure) at this location are presented, analyzed, and compared with a nearby public site in section 4. Then, turbulent kinetic energy and sensible heat flux annual variations are discussed in section 5 followed by concluding remarks.

2. RELATED WORK

Exchanges of moisture, heat, and momentum occur within the surface layer through turbulent

eddies and mixing in atmospheric boundary layer. These eddies influence the way in which lower-tropospheric thermodynamic and kinematic structures evolve [31]. Weather and climate models make use of atmospheric turbulence parameters, e.g. turbulent kinetic energy and sensible heat flux, to predict temperature and wind patterns [32]. These parameters are often obtained via turbulence models, used within climate models, that need to be tuned using experimental field data. The atmospheric turbulent characteristics in this work are obtained using data from high-speed sonic anemometer measurements at 20 Hz. First, the mean values of the instantaneous three-dimensional velocity are calculated from 30-minute data periods. Then, the wind direction, i.e. the streamwise velocity in *x* direction, is calculated, and all the velocity data is rotated in that direction accordingly. Velocity fluctuations for each velocity components (*u*, *v*, and *w*) are then calculated by subtracting the instantaneous velocity from that of their respected mean, that is $u' = u - \bar{u}$. Symbols *u*, *v*, and *w* are for instantaneous streamwise, transverse and vertical directions, respectively. The overbar indicates an averaging operator of the variable and the prime indicates the fluctuations about the mean value. Note that the mean velocity values in the transverse and vertical directions become zero after rotation by default. The turbulent flux of momentum (or shear stress) is defined as:

$$\tau = \rho u_*^2 = \rho\sqrt{\overline{u'w'}^2 + \overline{v'w'}^2} \ , \tag{1}$$

where ρ is the mean air density and u_* is the friction velocity. Drag coefficient C_d is then defined as:

$$C_d = \tau / \rho\bar{u}^2 = \left(u_* / \bar{u}\right)^2 . \tag{2}$$

Turbulent Kinetic Energy (TKE) is defined as:

$$TKE = \frac{1}{2}\left(\sigma_u^2 + \sigma_v^2 + \sigma_w^2\right), \tag{3}$$

where, $\sigma_i \left(i = u, v, w\right)$ is the normalized variances of fluctuations of the wind velocity components. Sensible heat flux is defined as:

$$H = \rho C_p \overline{w'T'} , \tag{4}$$

where T is the sonic temperature and C_p is specific heat of ambient air.

3. METHODOLOGY

3.1 Experimental Site and Instrument

Atmospheric measurement was conducted in the coastal region of Al Ghariyah, Qatar (26.08 N, 51.36 E), from August 2015 to September 2016. Qatar is located on the south of the Persian Gulf and surrounded by sea on all sides except for the Saudi Arabia border in the south, Fig. 1. The measurement site is located in the coastal region around 20 m (varies due to the tide) from the sea line. The landscape of the experimental site is comprised of mainly flat sand dunes (average height ~ 0.5 m) with very sparse small bushes and scrubs. Although there are a few low-level small (one room), historical buildings in the area, they are all located far from the measurement tower.

Atmospheric wind and temperature data are collected on a 9 m tower using sonic anemometers (CSAT3) mounted at heights of 3.2 m, 6.8 m, and 8.8 m above the surface along with a thermometer in the middle of the tower. A weather station (Davis Vantage Pro2) is also mounted on the top of the measurement tower that measures average wind velocity, temperature, humidity, and air pressure in 30-minute intervals. The sonic anemometers are directly facing north and collect the wind speed in three dimensions, along with sonic temperatures, at a 20 Hz sampling rate. The sonic data are acquired by the CR5000 data logger connected to the sonic anemometers and filtered using a median filter [33] to remove spikes and record the median value of seven points, as recommended by Starkenburg et al. [34]. Public NOAA data from a neighboring site, Al Ruwais region, 16 km Northwest of the measurement site is also collected and used to compare with the measurements of this work.

4. RESULTS AND DISCUSSION

4.1 Annual Weather Patterns

Three-dimensional atmospheric data was collected from September 2015 to June 2016 using the sonic anemometer probes and weather station on the tower. The 30-minute averaged value of diurnal wind speed, temperature, relative humidity (RH), and ambient pressure in this measurement campaign are shown in Fig. 2. The orange circle in this figure represents the mean value while the upper blue and the lower yellow

lines indicate the maximum and minimum, respectively, mean values at corresponding times of the day averaged for the entire test period.

Fig. 2a shows the average value of diurnal variations of wind speed in this measurement campaign. It shows an average diurnal value of ~4.7 m/s with an increasing trend from midnight, reaching its maximum around 14:00 and decreasing again until midnight. The averaged maximum diurnal velocity is around 12 m/s with its peak of 14.3 m/s around noon, while the averaged minimum value is almost zero at night. It is important to note that the diurnal mean wind velocity value is always more than 4 m/s, indicating a well-developed turbulent atmospheric layer at all times at the site. Furthermore, this average wind speed indicates a higher wind energy potential in Qatar. Fig. 2b shows that the averaged diurnal temperature with a mean of ~26^{o}C. The temperature increases from 7:00 to 10:00, maintains the high temperature until 15:00, then followed by a downward trend back to the low value around 6:00. The averaged maximum diurnal temperature (blue line) is 38^{o}C, reaching its peak value of 41^{o}C at 12:00, while its minimum is about 35^{o}C. This figure shows the minimum diurnal average temperature (yellow line) remains below 11^{o}C, with an averaged value of 9^{o}C, while the coldest point for the diurnal temperature is 7^{o}C at 4:00 (yellow line).

Fig. 2c shows that the mean diurnal averaged RH is around 70%, with the highest humidity at night and lowest humidity at noon, because of a stronger solar radiation. The maximum diurnal RH is always above 90% during the day while the minimum value of ~20% is from 9:00 to 15:00. As expected, there is an inverse correlation between the trends of the mean RH with that of the temperature; as the temperature increases from 7:00 to 10:00, the RH decreases. Fig. 2d shows the air pressure fluctuates around 101.3 kPa with no signification daily trend. The mean value for the maximum and minimum air pressure is 102.8 kPa and 99.6 kPa, respectively.

Note that environmental conditions of 100% humidity and a bulb temperature of 35 ^{o}C, or higher, for more than six hours may result in hyperthermia and is considered intolerable [35]. According to the temperature and humidity values shown in Fig. 2b and 2c, usual human outdoor activities is not recommended in these extreme conditions in Qatar. These inconveniences of outdoor activities can further result in difficulty for constructions and transportation, hence lower productivity.

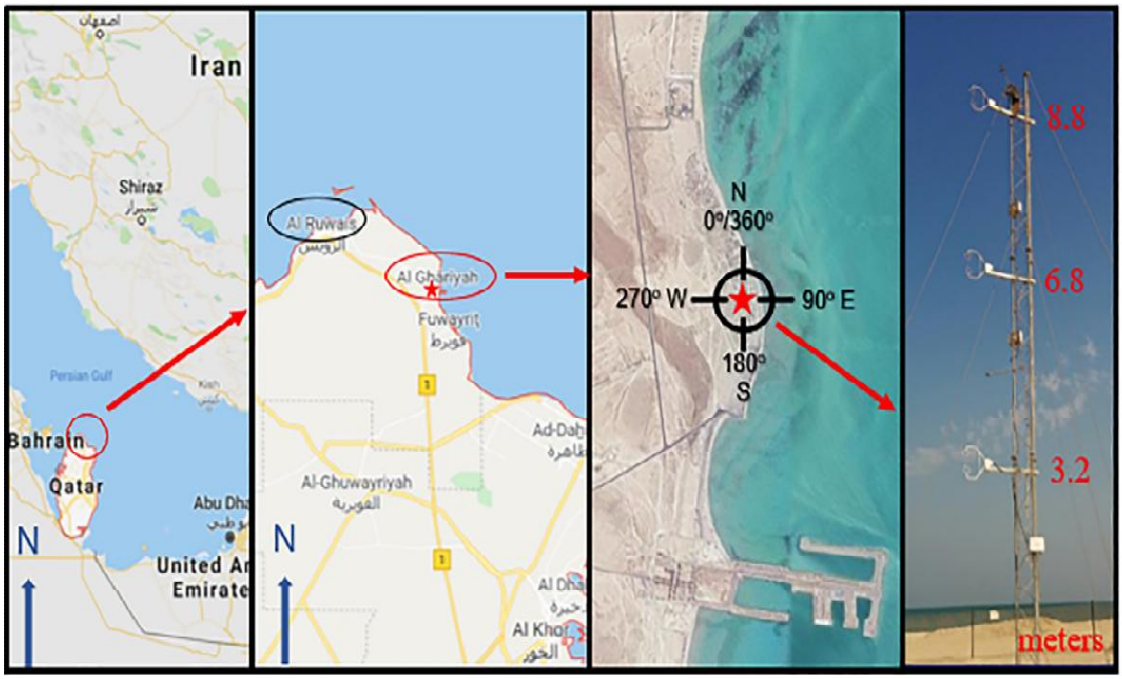

Fig. 1. Site location and View of the instrument tower

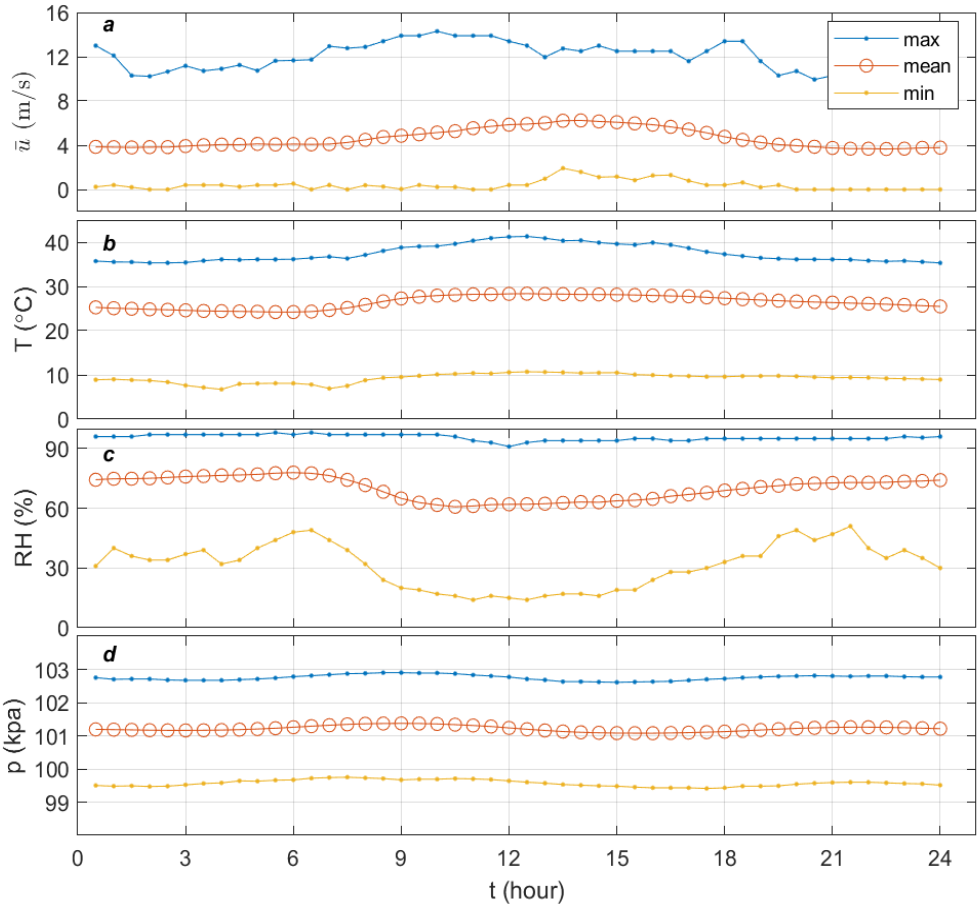

Fig. 2. Time-averaged diurnal variation of a) wind velocity, b) temperature, c) relative humidity, d) air pressure

Figs. 3, 4 and 5 show the daily averaged climate measurements in this work in comparison with the public data obtained in the neighboring "Al Ruwais" 16 km south-east of the measurement site. The error bars indicate the 95% confidence interval [36]. Data in Fig. 3 shows that velocity in the measurement site is slightly higher than that in the nearby coastal Al Ruwais site. This may be partly attributed to the fact that the velocity data in Al Ruwais is collected at a lower elevation (6 m). Fig. 4 shows a close agreement between the temperature values measured in the Al Ghariyah site and those of Al Ruwais site with an average yearly value of 26°C. It shows the daily average temperature is above 30°C during the hot days from May to October, while the daily averaged temperature for cool days is under 20°C from December to February [28]. Fig. 5a and 5b illustrate the relative daily averaged humidity and air pressure, respectively. The air pressure shows an opposite trend to that of the temperature; as the temperature decreases the pressure increases. The relative humidity shows a large scatter in the daily values with limited variance for the whole year, similar to that of the velocity data observed in Fig. 3 without a clear seasonal trend, with an annual mean value of 70%. Another important observation in this figure is the difference between the measured humidity values in Al Ghariyah and Al Ruwais sites, 16 km apart. It is important to recall that temperature and air pressure directly affect the value of local relative humidity. Since both these values are close to each other for the two sites, the observed difference between relative humidity is probably related to the difference in the wind direction relative to the coastline angle in the two sites. While the coastline of Al Ghariyah site runs north to south, almost 90 degrees from the horizontal line, Al Ruwais coastline runs northeast to southeast, around 45 degree from the horizontal line, Fig 1. Since the wind comes predominantly from the northwest, it reaches the measurement site, mostly, after

traveling over land whereas for Al Ruwais the wind directly comes from the sea.

Fig. 6 illustrates seasonal wind rose for the measurement campaign where the color variations represent the wind speeds from 0 to 14 m/s. This figure shows that the wind from Northwest is prevailing in all four seasons with an annual average speed of 4.7 m/s. Specifically, in fall, the wind mostly comes from northwest region with relative higher speeds than that from most of other direction except occasional gusts the east (seaside). In winter, high speed wind from northwest is dominating for most of the time. During this time, lower speed winds from the southeast take a much smaller portion of the chart compared to those of Fall. Spring has a similar wind distribution as winter, but northwest winds are of higher speed than that in winter. In summer, wind direction is more evenly distributes when compared to those of the other three seasons, but wind from northwest and west northwest still dominate this season. In summary, a dominant wind from northwest direction is observed for all duration of the year that is partly an indication of Shamal.

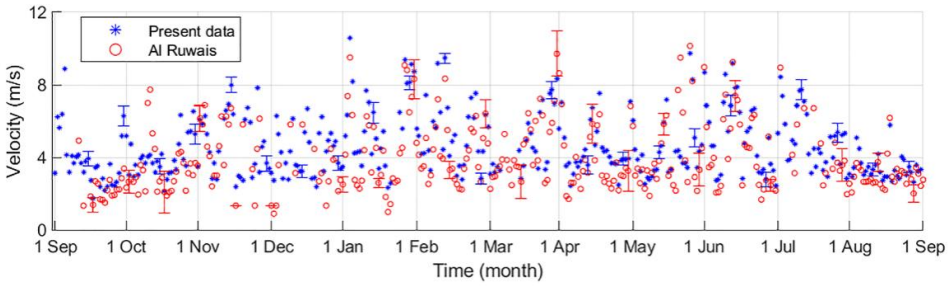

Fig. 3. Local velocity contrast with Al Ruwais from september 2015 to september 2016

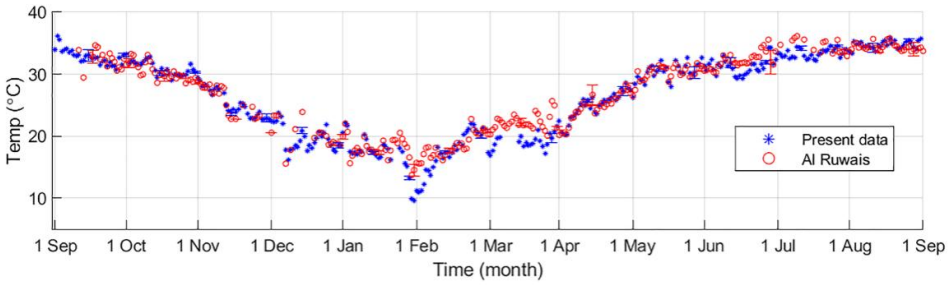

Fig. 4. Local temperature contrast with Al Ruwais from september 2015 to september 2016

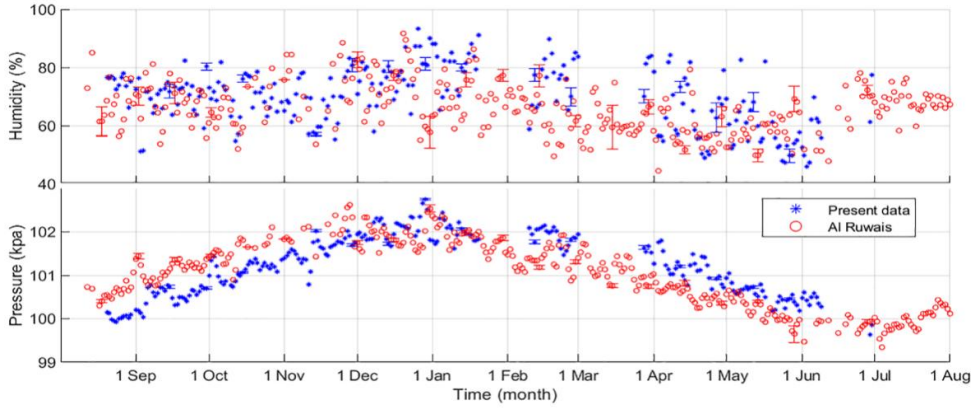

Fig. 5. Local relative humidity (top) and air pressure (bottom) in contrast with Al Ruwais

The specific wind phenomenon of 'Shamal' coming from Iraq over the Persian Gulf is a significant regional wind pattern, Fig. 7. A more commonly used definition of a "Shamal day" is a day with a wind speed of over 8.75 m/s (17 kn) and a meteorological direction between 270º and 360º for at least 3 hours of the day [24,37]. Fig. 6 shows that, in all seasons, the dominant northwest wind takes a large portion of the wind direction distribution. However, Shamal days were mostly observed in summer and winter during this measurement campaign due to more frequent occurrence of wind with speed larger than 4 m/s than the other two seasons. It is important to recall that the measured average wind velocity of 4.7 m/s indicate the potential for an abundant wind energy source [22] for a wind farm facing the northwest direction.

Fig. 8a shows a complete summary of wind velocity variations as a function of local time in this measurement campaign. This figure shows wind velocity is commonly high around noon and low at midnight. The wind velocity from the noon to afternoon period is relatively higher from January to March and from June to August compared to the other months. In the early morning, the highest and the lowest wind speeds occur in January and October, respectively. In the evening, the wind speed is lowest around 21:00 on most days, especially during the summertime. The higher wind velocity in the afternoon may be partially associated with sea breeze, wind from the offshore directions. However, a land breeze [38], a reverse wind from the onshore direction, mostly occurs at night due to the greater cooling rate of the land.

Fig. 8b shows the frequency distribution of 30 minute-mean wind velocity. This figure shows a general agreement with the commonly observed wind velocity frequency distribution, with a positive skewness. The peak frequency of the velocity distribution is observed to occur at 3-3.5 m/s range. Interestingly, this figure shows that only 27% of wind data in the year is less than 3 m/s and 43% of data occurs at a velocity of higher than the annual average of 4.6 m/s (the red line). The present data shows a higher wind energy potential in Qatar coast when compared with some other reported locations in the world. For example, the mean wind speed of no more than 5 m/s with the most frequent wind velocity of around 3 m/s is studied for wind energy application in Malaysia [39]. Considering the sunny climate in the region with minor precipitation, our result suggest that a hybrid power system [40,41] with both wind and solar energy can suits the Gulf coast (Qatar) environment.

The knowledge of ambient air temperature variations is of special interest for urban and industrial planning. For example, most electrical power in the Persian Gulf region is generated using gas turbine power plants where it is known that the efficiency of gas turbine power plants decreases with an increase in the inlet air temperature and relative humidity [42,43]. This is of critical importance in this region as the demand on electrical power peaks during times of high ambient air temperature due to the increased use of air conditioning [44]. Fig. 9a shows the measured monthly-daily mean temperature pattern in the measurement site. It shows that temperature is the highest around the noon period from 9:00 to 18:00, with the length of this period changes with the changing times of sunrise-sundown (change of season). The earliest sunrise time is 4:42 in the second half of June, and the latest is at 6:21 in the second half of December. The sunset time follows a similar cycle with the earliest sunset at16:43 and the latest sunset of 18:28. This corresponds to the shortest and longest day times, which are 10 hours and 33 minutes in December and 13 hours and 42 minutes in June, respectively. As shown in Fig. 9a, temperatures stay high from March to October, followed with a shorter, cool period from December to February. Meanwhile, the coolest time of the year is around sunrise during January and February. The temperature trends observed in this measurement campaign agrees with that of a typical subtropical coastal climate as previously reported for long term temperature patterns in Qatar [28]. Fig. 9b shows the frequency distribution of 30 minute-mean ambient temperature measurements in this campaign. This figure shows two distinct frequency peaks of 20^{o}C and 33^{o}C which correspond to warmer and cooler seasons of the year, respectively. The average temperature 27 ^{o}C is in the concave between the two peaks with 56% of data showing temperatures higher than the average value. Note that the shape of the distribution changes with the different binning time as shown by Saloranta et al. [45] for different frequency distributions of ambient air temperatures for 1, 3, 6, 12, and 24 hour averaging window.

Monthly mean pressure and relative humidity are illustrated in Figs. 10a and 11. Both figures show different diurnal trends from those of velocity and temperature shown in Figs. 8a and 9a,

respectively. Specifically, the air pressure trend shows an inverse pattern to that of the temperature, where the highest pressure is around 9:00 and 21:00 from December to February when the temperature is low. The relative humidity is low in the daytime, especially around noon, and high at night, especially around sunrise. The highest relative humidity exceeds 90% during the cool days of winter from December to March. Fig. 10b shows the frequency distribution of ambient daily humidity measurement the year. This figure shows that the humidity, in this coastal region, is negatively skewed with a peak humidity of about 80% where 55% of data are at higher humidity than the annual average value of 70%. The relative humidity values reported here are higher than the ones reported by Cheng et al. [28] because the present data was collected around 15 m from the sea which is much closer than that reported by Cheng et al.

4.2 Turbulent Characteristics

Basic turbulent characteristics of the atmospheric boundary layer (drag coefficient, TKE, and heat flux) are discussed in this section. Note that the current data does not show any significant daily, seasonal, or diurnal C_d pattern, hence it is not presented here. However, the relation between the drag coefficient relative to the wind direction at the measurement site are shown in Fig. 12. This figure shows relatively higher values of C_d for the wind coming from 270°-330°. This coincides with the dominant northwest wind direction shown in Fig. 6. This direction coincides with the Shamal, the higher magnitude of which results in a higher drag coefficient. Another reason may be the fact that this direction corresponds to the wind passing over land, experiencing a higher roughness than the wind passing over the sea from east side. The less crowded region at ~180° (South) corresponds to the blocked view of the tower; the sonic anemometers were installed facing north and wind coming from the south is excluded due to possible disturbance by the tower structure.

The monthly-daily mean TKE at the measurement site is shown in Fig. 13 at 9 m height from the ground. This figure shows that the TKE is higher during the day, especially around noon, and weak during the night, similar to the trend reported by Xia et al. [4] for Colorado City, TX. A higher turbulence intensity is observed around noon in late springtime, from May to July. This may be related to the increase in solar radiation at this time that increases the mixing process in the atmosphere causing a higher TKE. The trends in this figure are similar to those of the temperatures shown in Fig. 9a. Furthermore, TKE may also be related to the wind magnitude shown in Fig. 8a; a larger wind shear exists when the wind velocity is higher. Sensible heat flux is an indication of direct heat transfer between surface and atmosphere; it attains a positive value when heat is directed away from the surface toward the atmosphere. Fig.14 shows the monthly-daily sensible heat flux mean at 9 m above the ground in the year. During the day, the sensible heat flux is directed from the land surface to the air (positive sign) since the ground temperature is higher than the air above and is directed in the opposite direction during the night. The largest heat flux is recorded around noon from April to July, indicating a large temperature difference between land and air during this period. The largest negative heat flux magnitude is in the period between midnight and sunrise during January and June. For the periods around sunrise and sunset, the sensible heat flux is near zero, which indicates a thermally stable turbulent boundary layer when the temperature difference between the earth surface and the atmosphere is small.

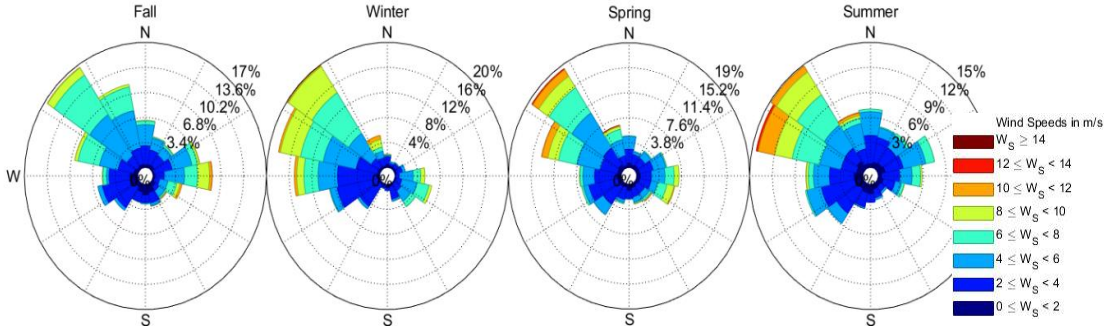

Fig. 6. Seasonal wind rose from fall 2015 (left) to summer 2016 (right)

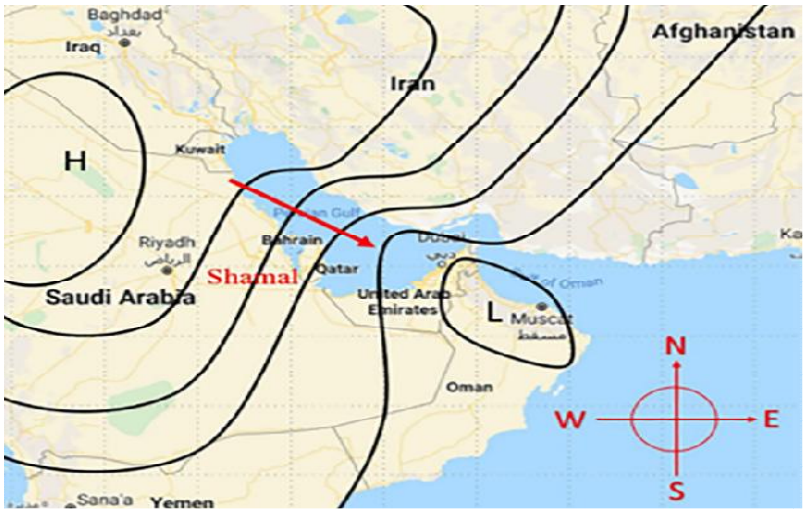

Fig. 7. Pressure pattern during Shamal in the Persian Gulf [23]

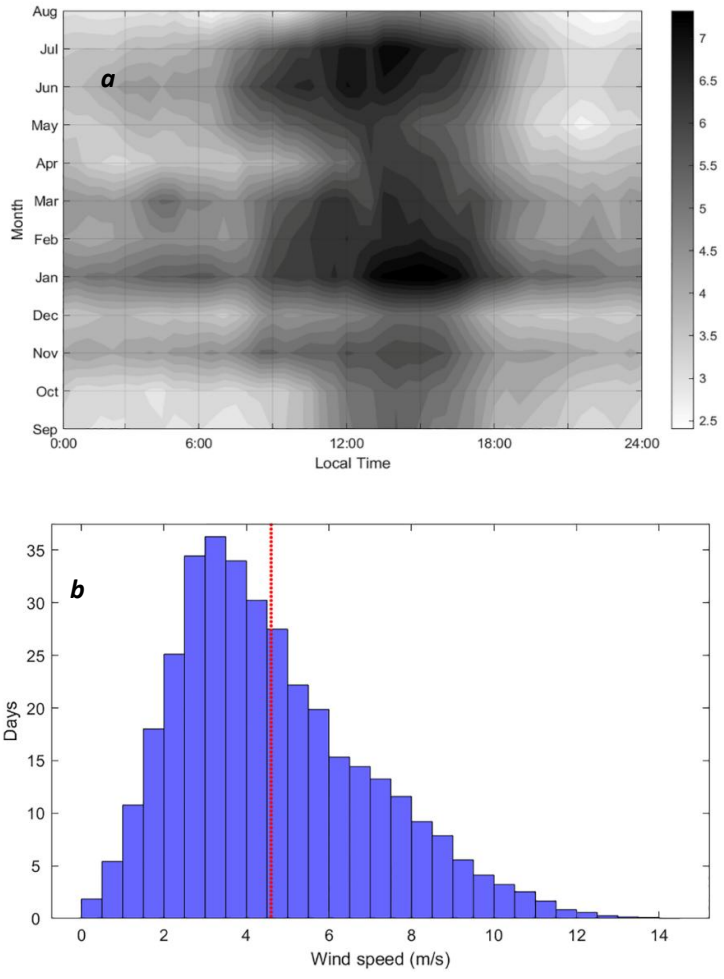

Fig. 8. a) Monthly mean velocity (m/s) magnitude variations and b) frequency distribution of 30-minutes mean wind speed at 9m height elevation

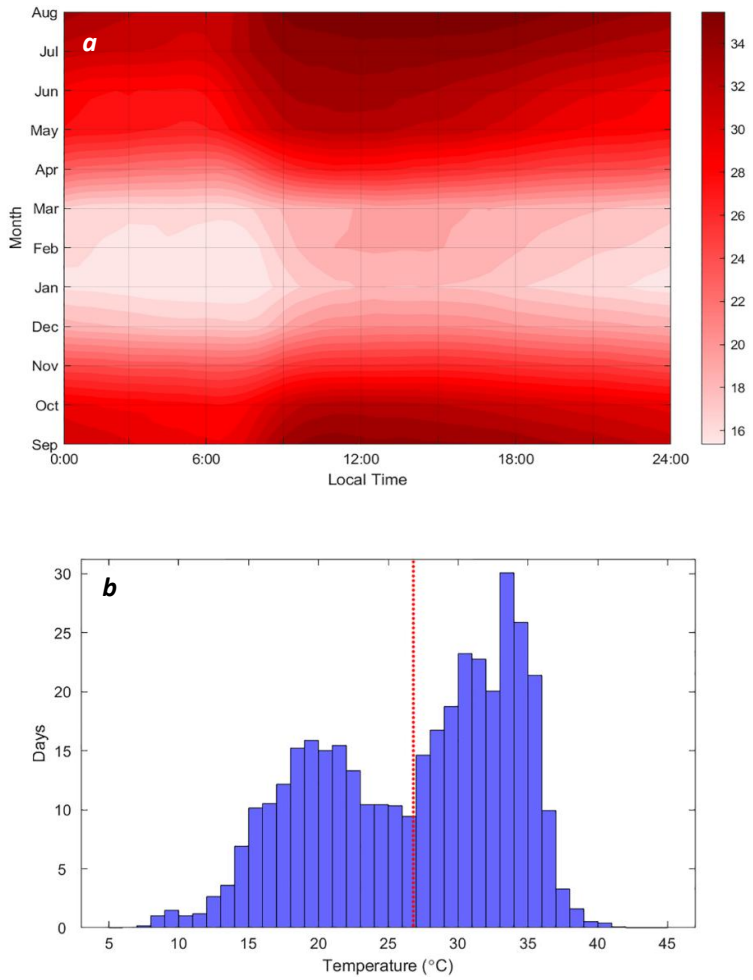

Fig. 9. a) Monthly mean temperature variations (°C) and b) 30 minute-mean ambient temperature frequency distribution of measured 9 m above ground

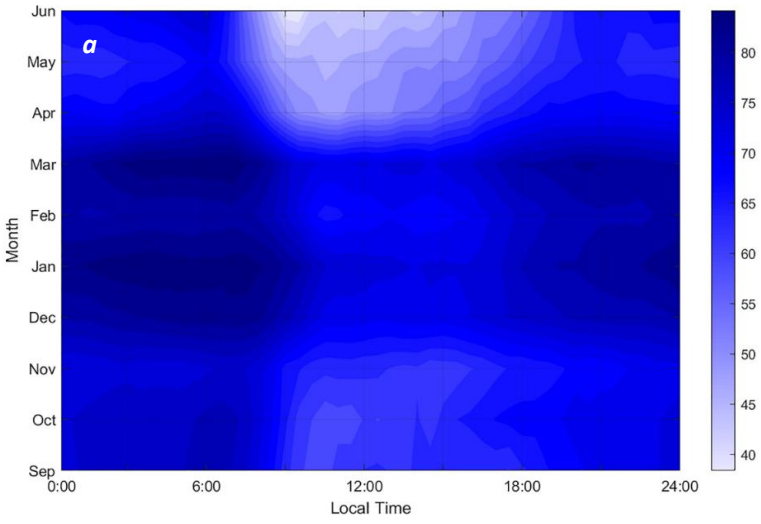

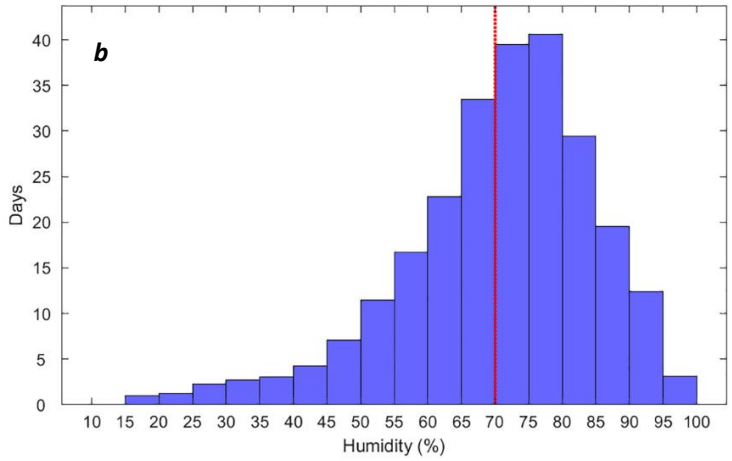

Fig. 10. a) Monthly mean relative humidity variations (%) and b) frequency distribution of 30-minutes mean relative humidity for the measurement period

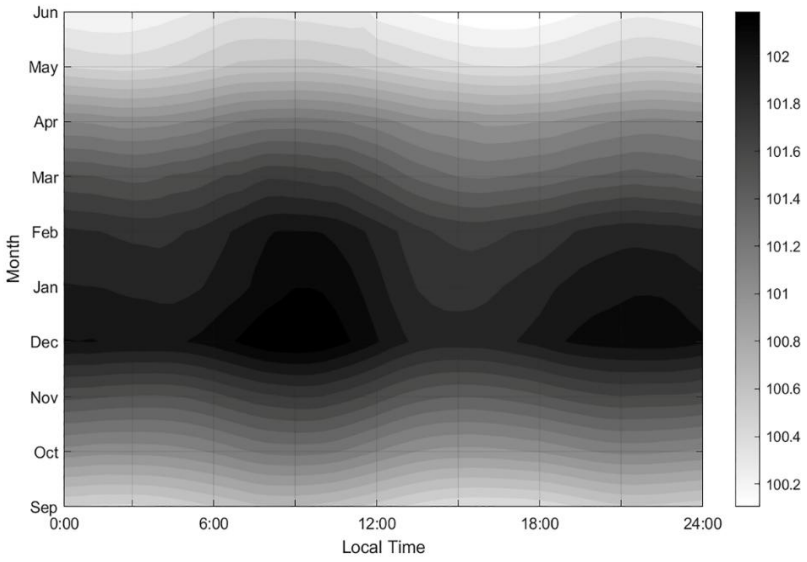

Fig. 11. Monthly mean pressure variations (kpa)

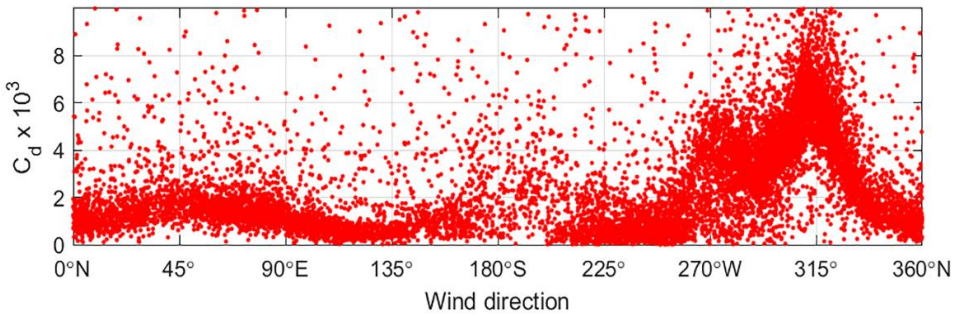

Fig. 12. Drag coefficient versus the wind direction September 2015 to August 2016

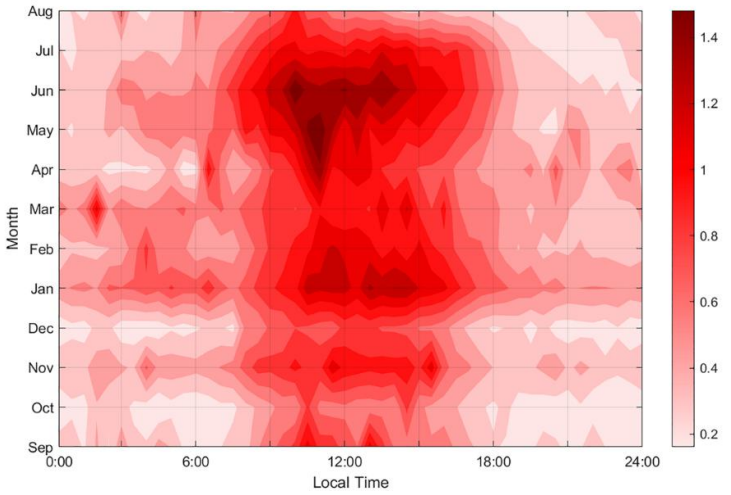

Fig. 13. Monthly mean TKE variations (m^2/s^2) at 9 m elevation

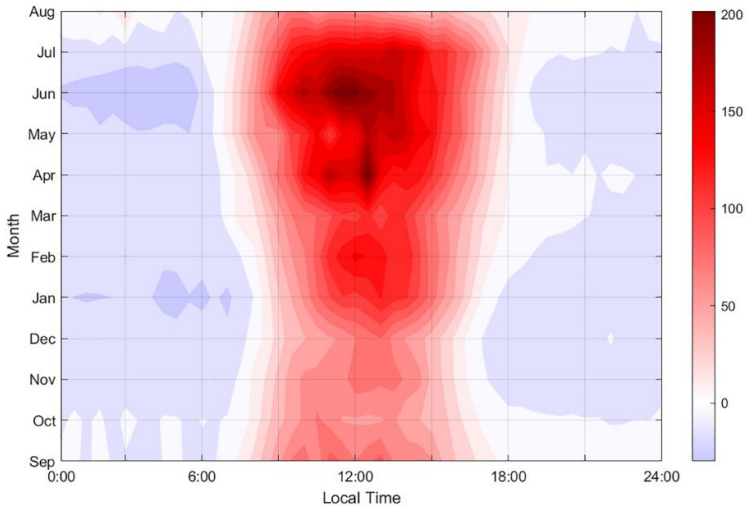

Fig. 14. Monthly mean heat flux variations (W/m^2) at 9 m elevation

5. CONCLUSION

This work reports the annual diurnal climate patterns in the coastal region of Qatar in the Persian Gulf (Al Ghariyah, 26.08 N, 51.36 E) from August 2015 to September 2016. The data was obtained from a low-speed weather station as well as a high-speed sonic anemometer at 9 m above the ground. The results show that the wind is dominant from the northwest with an average wind speed of 4.7 m/s, highlighting the potential of this location as an abundant wind energy source.

The average temperature, relative humidity, and air pressure during the test period are 26°C, 70% and 101.3 kpa, respectively. Wind velocity and temperature agrees with previously reported patterns of high values in the noon period and low at midnight, as shown in Fig. 8a and 9a. The air pressure shows an inverse diurnal trend from the temperature, and humidity, with a relatively low value in daytime, especially around noon, and relatively high at night, especially around sunrise.

Basic analysis of atmospheric turbulence at this location indicates that drag coefficient is relatively higher for the dominant northwest winds than for the other directions. This is partly because the path of this wind is over land for the measurement site. The TKE is strong during the day, especially

around noon, and weak during the night, which is aligned with the diurnal wind velocity and temperature patterns. Finally, the heat flux measurements indicate heat transfers from land to air during the day and vice versa during the night, with a thermally stable turbulent boundary layer at sunrise and sunset.

ACKNOWLEDGEMENT

This publication was made possible by NPRP grant # 5-543-2-220 from the Qatar National Research Fund (a member of Qatar Foundation). The statements made herein are solely the responsibility of the authors.

COMPETING INTERESTS

Authors have declared that no competing interests exist.

REFERENCES

1. Ferrero, Enrico, Stefano Alessandrini, Francois Vandenberghe. Assessment of planetary-boundary-layer schemes in the weather research and forecasting model within and above an urban canopy layer. Boundary-Layer Meteorology. 2018;168(2):289–319.
2. Mage, David T. Frequency distributions of hourly wind speed measurements. Atmospheric Environment. 1980;14(3):367–74.
3. Wang, Lingzhi, Jun Liu, Fucai Qian. Frequency Distribution Model Ofwind Speed Based on the Exponential Polynomial for Wind Farms. Sustainability (Switzerland). 2019;11(3).
4. Xia, Geng, Liming Zhou, Jeffrey M. Freedman, Somnath Baidya Roy, Ronald A. Harris, Matthew Charles Cervarich. A case study of effects of atmospheric boundary layer turbulence, wind speed, and stability on wind farm induced temperature changes using observations from a field campaign. Climate Dynamics. 2016;46(7–8):2179–96.
5. Dupont JC, Haeffelin M, Badosa J, Elias T, Favez O, Petit JE, Meleux F, Sciare J, Crenn V, Bonne JL. Role of the boundary layer dynamics effects on an extreme air pollution event in Paris. Atmospheric Environment. 2016;141:571–79.
6. Ashfaqur Rahman, Mansour Almazroui M, Nazrul Islam M, Enda O'Brien, Ahmed Elsayed Yousef. The role of land surface fluxes in Saudi-KAU AGCM: Temperature climatology over the arabian peninsula for the period 1981–2010. Atmospheric Research. 2018;200:139–52.
7. Sherwood, Steven C, William Ingram, Yoko Tsushima, Masaki Satoh, Malcolm Roberts, Pier Luigi Vidale, Paul A. O'Gorman. Relative humidity changes in a warmer climate. Journal of Geophysical Research Atmospheres. 2010;115(9):1–11.
8. Alsarmi, Said Hamed, Richard Washington. Changes in climate extremes in the arabian peninsula: analysis of daily data. International Journal of Climatology. 2014;34(5):1329–45.
9. Schmidt Daniel F, Kevin M. Grise. The response of local precipitation and sea level pressure to hadley cell expansion. Geophysical Research Letters. 2017;44(20):10,573-10,582.
10. Ehsan, Muhammad Azhar, Dario Nicolì, Fred Kucharski, Mansour Almazroui, Michael K. Tippett, Alessio Bellucci, Paolo Ruggieri, In Sik Kang. Atlantic ocean influence on middle east summer surface air temperature. Npj Climate and Atmospheric Science. 2020;3(1):1–8.
11. Michael Reynolds R. Physical oceanography of the gulf, strait of hormuz, and the gulf of oman-results from the mt mitchell expedition. Marine Pollution Bulletin. 1993;27(C):35–59.
12. Sheppard, Charles, Mohsen Al-Husiani, Al-Jamali F, Faiza Al-Yamani, Rob Baldwin, James Bishop,et al. The gulf: A young sea in decline. Marine Pollution Bulletin. 2010;60(1):13–38.
13. Xue, Pengfei, Elfatih A, Eltahir B. Estimation of the heat and water budgets of the persian (Arabian) gulf using a regional climate model. Journal of Climate. 2015;28(13):5041–62.
14. Zhang, Xuebin, Enric Aguilar, Serhat Sensoy, Hamlet Melkonyan, Umayra Tagiyeva, Nader Ahmed, Nato Kutaladze,et al. Trends in middle east climate extreme indices from 1950 to 2003. Journal of Geophysical Research Atmospheres. 2005;110(22):1–12.
15. Almazroui, Mansour, M. Nazrul Islam, Jones PD, Athar H, Ashfaqur Rahman M. recent climate change in the arabian peninsula: seasonal rainfall and temperature climatology of Saudi Arabia for 1979-2009. Atmospheric Research. 2012;111:29–45. 247-264.

16. Almazroui, Mansour, M. Salman Khalid, M. Nazrul Islam, Sajjad Saeed. Seasonal and regional changes in temperature projections over the Arabian peninsula based on the CMIP5 Multi-Model ensemble dataset. Atmospheric Research. 2020;239:104913.
17. Teather, Kevin, Natacha Hogan, Kim Critchley, Mark Gibson, Susanne Craig, Janet Hill. Examining the links between air quality, climate change and respiratory health in qatar. Avicenna. 2013;9.
18. Al Senafi, Fahad, Ayal Anis. Shamals and climate variability in the northern Arabian/Persian Gulf from 1973 to 2012. International Journal of Climatology. 2015;35(15):4509–28.
19. Jish Prakash P, Stenchikov G, Kalenderski S, Osipov S, Bangalath H. The impact of dust storms on the Arabian peninsula and the red sea. Atmospheric Chemistry and Physics. 2015;15(1):199–222.
20. Farahat, Ashraf. Air pollution in the Arabian peninsula (Saudi Arabia, the United Arab Emirates, Kuwait, Qatar, Bahrain, and Oman): causes, effects, and aerosol categorization." Arabian Journal of Geosciences. 2016;9(3).
21. Kamranzad, Bahareh, Amir Etemad-Shahidi, Vahid Chegini, Abbas Yeganeh-Bakhtiary. Climate change impact on wave energy in the persian gulf. Ocean Dynamics. 2015;65(6):777–94.
22. Yip, Chak Man Andrew, Udaya Bhaskar Gunturu, Georgiy L. Stenchikov. Wind resource characterization in the Arabian Peninsula. Applied Energy. 2016;164:826–36.
23. Perrone, Thomas J. Winter shamal in the persian gulf. Monterey, California; 1979.
24. Rao, Govinda P, Mohammed Al-Sulaiti, Ali Hamid Al-Mulla. Winter shamals in qatar, Arabian Gulf. Weather. 2001;56(12):444–51.
25. Ramli, Makbul AM, Ssennoga Twaha, Abdulaziz U. Alghamdi. Energy production potential and economic viability of grid-connected wind/pv systems at Saudi Arabian coastal areas. Journal of Renewable and Sustainable Energy. 2017;9(6):1–24.
26. Singha, Arindam, Reza Sadr. Characteristics of surface layer turbulence in coastal area of qatar." Environmental Fluid Mechanics. 2012;12(6):515–31.
27. Makido, Yasuyo, Vivek Shandas, Salim Ferwati, David Sailor. Daytime variation of urban heat islands: The case study of Doha, Qatar. Climate. 2016;4(2):1–14.
28. Cheng, Way Lee, Ayman Saleem, Reza Sadr. Recent warming trend in the coastal region of qatar. Theoretical and Applied Climatology. 2017;128(1–2):193–205.
29. Othman, Nadzri, Mohd Zubir Mat Jafri, Lim Hwee San. Estimating particulate matter concentration over arid region using satellite remote sensing: A case study in Makkah, Saudi Arabia. Modern Applied Science. 2010;4(11):131–42.
30. Smith, Adam, Neal Lott, Russ Vose. The integrated surface database: recent developments and partnerships. Bulletin of the American Meteorological Society. 2011;92(6):704–8.
31. Cohen, Ariel E, Steven M. Cavallo, Michael C. Coniglio, Harold E. Brooks. A review of planetary boundary layer parameterization schemes and their sensitivity in simulating southeastern U.S. Cold Season Severe Weather Environments. Weather and Forecasting. 2015;30(3):591–612.
32. Liu, Gang, Yangang Liu, Satoshi Endo. Evaluation of surface flux parameterizations with long-term ARM observations. Monthly Weather Review. 2013;141(2):773–97.
33. Brock, Fred V. A nonlinear filter to remove impulse noise from meteorological data. Journal of Atmospheric and Oceanic Technology. 1986;3(1):51–58.
34. Starkenburg, Derek, Stefan Metzger, Gilberto J. Fochesatto, Joseph G. Alfieri, Rudiger Gens, Anupma Prakash, Jordi Cristóbal. Assessment of despiking methods for turbulence data in micrometeorology. Journal of Atmospheric and Oceanic Technology. 2016;33(9):2001–13.
35. Pal JS, Eltahir EAB. Future temperature in southwest Asia projected to exceed a threshold for human adaptability. Nature Climate Change. 2016;6(2):197–200.
36. Benedict LH, Gould RD. Towards better uncertainty estimates for turbulence statistics. Experiments in Fluids. 1996;22(2):129–136.
37. Rao, Govinda P, Hatwar HR, Mohammed Hassan Al-Sulaiti, Ali Hamid Al-Mulla. Summer shamals over the Arabian gulf. Weather. 2003;58(11):428–34.

38. Masouleh Z, Walker D, Crowther J. Sea breeze characteristics on two sides of a shallow gulf: Study of the Gulf St Vincent in South Australia. Meteorological Applications. 2016;23(2):222– 229.
39. Kadhem AA, Wahab NIA, Abdalla AN. Wind energy generation assessment at specific sites in a Peninsula in Malaysia based on reliability indices. Processes. 2019;7(7).
40. Abdalla AN, Nazir MS, Jiang MX, Kadhem AA, Wahab NIA, Cao S, Ji R. Metaheuristic searching genetic algorithm based reliability assessment of hybrid power generation system. Energy Exploration and Exploitation. 2021;39(1):488–501.
41. Nazir MS, Abdalla AN, Wang Y, Chu Z, Jie J, Tian P, Jiang M, Khan I, Sanjeevikumar P, Tang Y. Optimization configuration of energy storage capacity based on the microgrid reliable output power. *Journal of Energy Storage*. Elsevier, 2020;32:101866.
42. Liebendorfer, Kurt M, John S. Andrepont. Cooling the hot desert wind: turbine inlet cooling with thermal energy storage (tes) increases net power plant output 30%. ASHRAE Transactions 111 Part. 2005;2:545–50.
43. Alasfour FN, Al-Fahed SF, Abdulrahim HK. The effect of elevated inlet air temperature and relative humidity on Gas Turbine cogeneration system: exergy assessment. Int. J. Exergy. 2011;8(3) .
44. Alhazmy MM, Jassim RK, Zaki GM. Performance enhancement of gas turbines by inlet air-cooling in hot and humid climates. Int. J. Exergy Res. 2006;30:777-797.
45. Saloranta T, Thapa A, Kirkham JD, Koch I, Melvold K, Stigter E, Litt M, Møen K. A model setup for mapping snow conditions in high-mountain himalaya. Frontiers in Earth Science; 2019.

Peer-review history:
The peer review history for this paper can be accessed here:
http://www.sdiarticle4.com/review-history/66402